



## Short Communication

Quinoline appended pillar[5]arene (QPA) as Fe<sup>3+</sup> sensor and complex of Fe<sup>3+</sup> (FeQPA) as a selective sensor for F<sup>-</sup>, arginine and lysine in the aqueous mediumRoymon Joseph<sup>a,\*</sup>, Adersh Asok<sup>b</sup>, Kuruvilla Joseph<sup>a</sup><sup>a</sup> Department of Chemistry, Indian Institute of Space Science and Technology (IIST), Thiruvananthapuram, Kerala 695547, India<sup>b</sup> Material Science and Technology Division, National Institute for Interdisciplinary Science and Technology (NIIST), Thiruvananthapuram 695019, India

## ARTICLE INFO

## Article history:

Received 11 June 2019

Received in revised form 7 July 2019

Accepted 14 July 2019

Available online 16 July 2019

## Keywords:

Fe<sup>3+</sup> sensor

Fluoride sensor

Pillar[5]arene

Amino acid detection

Fluorescence

## ABSTRACT

A quinoline functionalized pillar[5]arene, **QPA** has been prepared and its interaction with biologically relevant ions and molecules in aqueous solution has been demonstrated. The sensor molecule, **QPA** has shown selectivity towards Fe<sup>3+</sup> among eleven metal ions studied. The Fe<sup>3+</sup> complex of **QPA** (**FeQPA**) selectively interacts with F<sup>-</sup> among halides by ~4 fold fluorescence enhancement. Further, **FeQPA** has shown selectivity towards arginine and lysine among twenty naturally occurring amino acids. The binding of **QPA** with Fe<sup>3+</sup> has been confirmed by MALDI-TOF and <sup>1</sup>H NMR titrations.

## 1. Introduction

Owing to the indispensable role in various biological processes, the detection and quantification of ions and molecules are of fundamental importance [1,2]. To cite an example; iron the most essential trace element in the human body plays an integral role in many physiological processes such as oxygen transport, electron transfer, and enzyme catalysis [3–8]. The optimum amount of iron present in men and women are 3 and 4 g respectively and the total iron is disseminated throughout the body in haemoglobin, bone marrow, tissues, muscles, blood proteins, etc. [9]. Iron deficiency or overload may impact various biological processes in human body and this abnormal iron content may lead to different diseases such as anemia, Parkinson's syndrome, Alzheimer's disease, and cancer [10,11]. Consequently, the monitoring of iron levels in humans using fluorescent molecules has been elevated to an intriguing area of research in recent years [12–14]. Also, due to the relevance of anions in chemical, biological, and environmental processes several synthetic receptors have been reported in the literature for the selective sensing of anions [15,16]. Among various anions, detection of F<sup>-</sup> is of particular concern on account of its vital role in treating osteoporosis and protecting dental health [17]. Nevertheless, excessive fluoride ingestion may lead to urolithiasis and fluorosis [18]. Thus the detection of F<sup>-</sup> is paramount in human health.

In addition to cations and anions, amino acids are involved in several crucial functions in cell regulations and metabolism, and they are essential in numerous cellular functions [19,20]. For instance, the basic amino acids such as arginine and lysine play a vital role in the proper functioning of biological systems. Arginine functions as a precursor for the synthesis of agmatine, creatine, glutamate, urea, proline, nitric oxide and polyamines [21,22]. The important biological processes associated with arginine are tissue integrity, reproduction, hormone release, wound healing, etc. [23,24]. The ability of arginine to lower blood pressure, reduce blood clots and strokes and its application in the treatment of erectile dysfunction is well evident from the literature [25,26]. Arginine overdose may lead to life threatening allergic reactions, anaphylaxis and increase in the levels of stomach acid [22]. Similarly, lysine also plays vital role in various biological processes. However, it acts as a precursor for protein synthesis and in the biosynthesis of carnitine. Excess amount of lysine in plasma and urine may cause congenital metabolic disorders such as cystinuria or hyperlysinemia [23,27,28]. Therefore, the selective detection of ions and molecules are of necessity in biology to avert its deficiency or overload and thereby head off several side effects in humans [23,24,29–31].

Though there are several synthetic fluorescent receptors known for the selective detection of ions and amino acids, a single system which recognizes all the three species; cations, anions and amino acids are rather rare [32,33]. In the search for a suitable molecular system which can function as a platform for functionalization, ease of synthesis, tuning solubility, hydrophobic and hydrophilic cavity we have come

\* Corresponding author.  
E-mail address: [royj80@gmail.com](mailto:royj80@gmail.com) (R. Joseph).

across a relatively new supramolecular system, pillar[5]arenes. Pillar[*n*]arenes are first reported by Ogoshi and co-workers in 2008 and the functionalized pillar[*n*]arenes are known for various applications in the areas of host-guest recognition, fluorescence sensing, supramolecular aggregates, biomedical applications, etc. [34–41]. Hence, in this paper we have demonstrated the synthesis of a novel quinolone appended pillar[5]arene (**QPA**) through a triazole linkage and its selective detection of Fe<sup>3+</sup> using fluorescence spectroscopy. Further, the iron complex of **QPA** (**FeQPA**) has been used for the sensing of F<sup>−</sup> among all the halides and arginine and lysine among the twenty naturally occurring amino acids by fluorescence spectroscopy.

## 2. Experimental section

### 2.1. Materials and physical methods

The salts used for the present study, viz., Mn(ClO<sub>4</sub>)<sub>2</sub>·6H<sub>2</sub>O, Fe(ClO<sub>4</sub>)<sub>2</sub>·xH<sub>2</sub>O, Fe(ClO<sub>4</sub>)<sub>3</sub>·6H<sub>2</sub>O, Co(SO<sub>4</sub>)<sub>2</sub>·7H<sub>2</sub>O, Ni(ClO<sub>4</sub>)<sub>2</sub>·6H<sub>2</sub>O, Cu(ClO<sub>4</sub>)<sub>2</sub>·6H<sub>2</sub>O, Zn(ClO<sub>4</sub>)<sub>2</sub>·6H<sub>2</sub>O, NaClO<sub>4</sub>·H<sub>2</sub>O, KClO<sub>4</sub>, Ca(ClO<sub>4</sub>)<sub>2</sub>·4H<sub>2</sub>O and Mg(ClO<sub>4</sub>)<sub>2</sub>·6H<sub>2</sub>O, were procured from Sigma Aldrich Chemical Company. Salts of anions, viz., Bu<sub>4</sub>NF and Me<sub>4</sub>NCl were procured from Otto Chemie Pvt. Ltd. and Bu<sub>4</sub>NBr, Bu<sub>4</sub>NI were procured from Spectrochem Pvt. Ltd. India. All the 20 naturally occurring amino acids, except lysine (TCI Chemicals (India) Pvt. Ltd.) and histidine (Avra Synthesis Pvt. Ltd. India), were procured from Spectrochem Pvt. Ltd. India. <sup>1</sup>H and <sup>13</sup>C NMR spectra were measured on a Bruker Ascend™ 400 spectrometer working at 400 MHz. The mass spectra were recorded on Bruker UltrafleXtreme MALDI-TOF mass spectrometer. The absorption and steady-state fluorescence spectra were measured on Varian Cary 100 Bio and Horiba Scientific FluoroMaz-4 respectively. The elemental analysis was carried out using PerkinElmer 2400 SeriesII CHNS.

### 2.2. General procedure for fluorescence experiments

All the fluorescence titrations were carried out in HPLC grade solvents. The bulk solution of **QPA** (6 × 10<sup>−4</sup> M) was prepared in DMSO and the salts of cations and anions, and the amino acids were dissolved in water. During the fluorescence titration the final concentration of **QPA** was kept at 10 μM and the concentration of metal salts was increased gradually to get requisite mole ratios of **QPA**:M<sup>n+</sup>. All the titrations were conducted in 1:1 H<sub>2</sub>O:CH<sub>3</sub>CN solvent. The limit of detection (LOD) was calculated from the fluorescence titration of host and guest species. The standard deviation of the blank (σ) was determined by measuring the fluorescence intensity of the probe without analyte at least 10 times. Then, the fluorescence intensity of the probe has been measured upon addition of increasing concentrations of analyte (3 times). The slope of the linearity plot (*m*) has been obtained by plotting the average value of fluorescence intensity of the probe versus concentration of analyte. Finally the LOD was calculated using the equation, LOD = 3σ/*m*.

### 2.3. Synthesis of QPA and its precursors

#### 2.3.1. Synthesis of **1a**

A mixture of hydroquinone (5.0 g, 45 mmol), potassium carbonate (28.2 g, 0.20 mol) and 1,6-dibromohexane (21 mL, 0.14 mol) in acetone (120 mL) were refluxed for 24 h under nitrogen atmosphere. The reaction mixture was cooled to 25 °C, filtered and the filtrate was evaporated under vacuum. The product was purified by chromatography (silica gel; petroleum ether/dichloromethane) followed by recrystallization from ethyl acetate to afford **1a** (8.2 g, 43%) as white solid. <sup>1</sup>H NMR (CDCl<sub>3</sub>): δ = 6.81 (s, 4H, ArH), 3.90 (t, *J* = 6.3 Hz, ArOCH<sub>2</sub>, 4H), 3.42 (t, *J* = 6.3 Hz, CH<sub>2</sub>Br, 4H), 1.92–1.85 (m, CH<sub>2</sub>, 4H), 1.80–1.73 (m, CH<sub>2</sub>, 4H), 1.54–1.44 (m, CH<sub>2</sub>, 8H) ppm. <sup>13</sup>C NMR (100 MHz): δ 153.2, 115.5, 68.4, 33.9, 32.8, 29.3, 28.0, 25.4 ppm. HRMS (ESI) calcd for C<sub>18</sub>H<sub>30</sub>Br<sub>2</sub>O<sub>2</sub> ([M + Na]<sup>+</sup>) 459.03332, found 459.03399.

#### 2.3.2. Synthesis of **1b**

To a solution of **1a** (6.3 g, 14.4 mmol) and paraformaldehyde (1.37 g, 45.6 mmol) in dichloroethane (120 mL) was added BF<sub>3</sub>·OEt<sub>2</sub> (2.0 mL, 15.9 mmol) under inert atmosphere and the reaction mixture was stirred at 25 °C for 2 h. Water (200 mL) was then added and the organic layer was separated. The solution was again extracted with dichloromethane (2 × 50 mL) and the combined organic layers were washed with water (2 × 100 mL), brine (2 × 100 mL) and dried with Na<sub>2</sub>SO<sub>4</sub> and the solvents evaporated. The product was purified by column chromatography (silica gel; petroleum ether/dichloromethane) to afford **1b** (3.1 g, 48%) as white solid. <sup>1</sup>H NMR (CDCl<sub>3</sub>): δ 6.87 (s, ArH, 10H), 3.91 (br, OCH<sub>2</sub>, 20H), 3.76 (s, ArCH<sub>2</sub>Ar, 10H), 3.24 (br, CH<sub>2</sub>Br, 20H), 1.81–1.60 (br, CH<sub>2</sub>, 40H), 1.44–1.28 (br, CH<sub>2</sub>, 40H) ppm. <sup>13</sup>C NMR (100 MHz): δ 149.6, 128.2, 114.6, 68.0, 33.9, 32.6, 29.8, 29.5, 28.1, 25.5 ppm. Anal. Calcd for C<sub>95</sub>H<sub>140</sub>Br<sub>10</sub>O<sub>10</sub>·12.7H<sub>2</sub>O: C, 46.2; H, 6.75. Found C, 45.96; H, 6.51.

#### 2.3.3. Synthesis of **1c**

Sodium azide (0.73 g, 11 mmol) was added to a solution of **1b** (2.0 g, 0.89 mmol) in DMF (30 mL) under inert atmosphere and the reaction mixture was kept at 90 °C for 12 h. After cooling to 25 °C, water (150 mL) was added and the precipitate was filtered and dried under vacuum to afford **1c** as white solid (1.5 g, 87%). <sup>1</sup>H NMR (400 MHz, CDCl<sub>3</sub>): δ 6.86 (s, ArH, 10H), 3.89 (br, ArOCH<sub>2</sub>, 20H), 3.76 (s, ArCH<sub>2</sub>Ar, 10H), 3.10 (br, CH<sub>2</sub>N<sub>3</sub>, 20H), 1.81 (br, CH<sub>2</sub>, 20H), 1.47–1.32 (m, CH<sub>2</sub>, 60H) ppm. <sup>13</sup>C NMR (100 MHz): δ 149.7, 128.3, 114.7, 68.1, 51.4, 29.8, 29.5, 28.7, 26.6, 25.9 ppm. Anal. Calcd for C<sub>95</sub>H<sub>140</sub>N<sub>30</sub>O<sub>10</sub>·5.6C<sub>3</sub>H<sub>7</sub>ON: C, 59.11; H, 7.95; N, 21.95. Found C, 58.58; H, 8.01; N, 22.48.

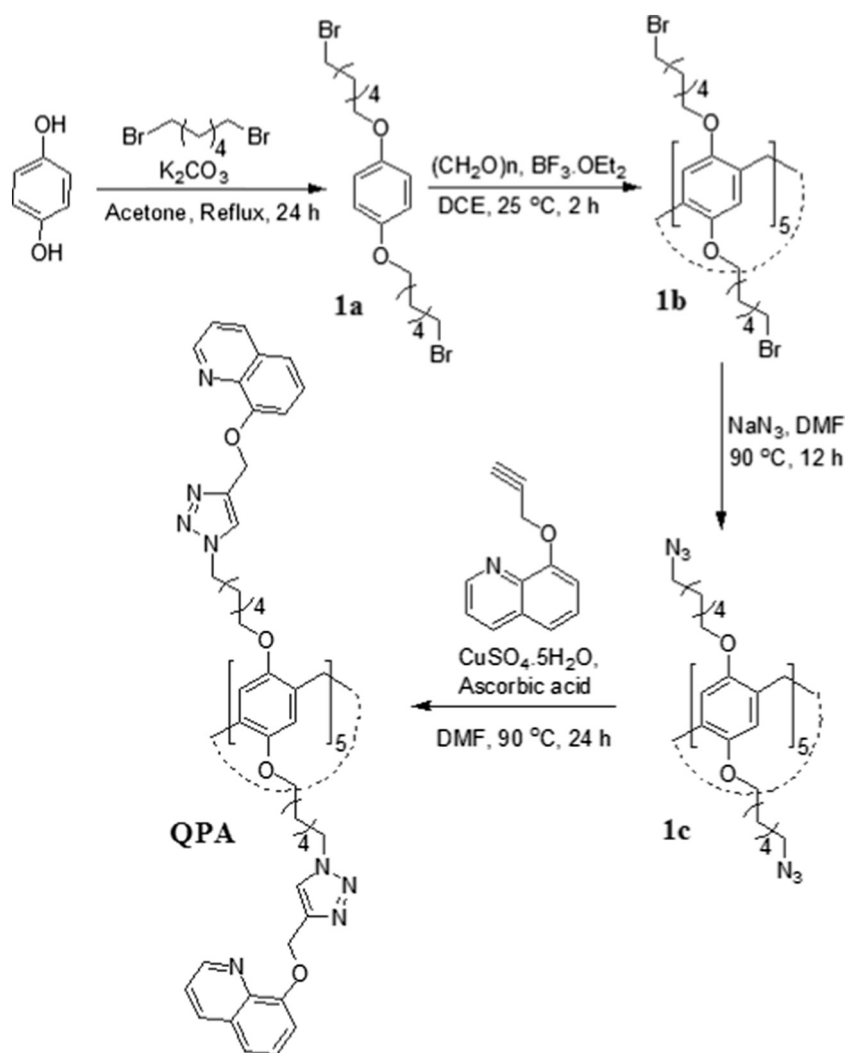
#### 2.3.4. Synthesis of **QPA**

A mixture of **1c** (0.25 g, 0.13 mmol), 8-(prop-2-ynoxy)quinoline [42] (0.37 g, 2.0 mmol), CuSO<sub>4</sub>·5H<sub>2</sub>O (8.0 mg, 32 μmol) and ascorbic acid (42 mg, 0.21 mmol) in DMF (25 mL) were kept at 90 °C for 24 h. The reaction mixture was cooled to 25 °C and evaporated. The solid was treated with water and extracted with dichloromethane (2 × 100 mL). The combined organic layers were washed with brine (2 × 20 mL) and dried with Na<sub>2</sub>SO<sub>4</sub> and the solvents evaporated. The product was purified by chromatography (silica gel; dichloromethane/methanol) to afford **QPA** as brown solid (0.31 g, 63%). <sup>1</sup>H NMR (400 MHz, CDCl<sub>3</sub>): δ 8.77 (br, ArH, 10H), 8.26 (m, ArH, 20H), 7.47–7.43 (m, ArH, 30H), 7.34–7.32 (m, ArH, 10H), 6.78 (s, ArH, 10H), 5.28 (s, OCH<sub>2</sub>, 20H), 4.35 (t, *J* = 6.8 Hz, OCH<sub>2</sub>, 20H), 3.95 (br, ArCH<sub>2</sub>Ar, 10H), 3.63 (br, NCH<sub>2</sub>, 20H), 1.83–1.69 (m, CH<sub>2</sub>, 40H), 1.49–1.46 (m, CH<sub>2</sub>, 20H), 1.31–1.28 (m, CH<sub>2</sub>, 20H) ppm. <sup>13</sup>C NMR (100 MHz): δ 154.3, 149.5, 149.3, 142.9, 140.2, 136.2, 129.5, 128.3, 127.1, 125.0, 122.3, 120.4, 114.4, 110.4, 68.2, 62.3, 49.8, 30.1, 29.5, 29.2, 26.3, 25.7 ppm. Anal. Calcd for C<sub>215</sub>H<sub>230</sub>N<sub>40</sub>O<sub>20</sub>·10CH<sub>2</sub>Cl<sub>2</sub>·10C<sub>3</sub>H<sub>7</sub>ON: C, 58.07; H, 6.11; N, 13.28. Found C, 57.74; H, 6.47; N, 13.61.

## 3. Results and discussion

The receptor molecule **QPA** has been synthesized by four known steps starting from commercially available material hydroquinone as given in Scheme 1. Alkylation of hydroquinone was carried out with 1,6-dibromohexane using potassium carbonate in acetone to afford dibromo derivative, **1a**. The cyclized derivative of pillar[5]arene, **1b** was obtained by the reaction of **1a** with paraformaldehyde and boron trifluoride diethyletherate in dichloroethane. Reaction of **1b** with sodium azide resulted in the formation of azido derivative of pillar[5]arene, **1c**. Finally, the sensor molecule, **QPA** was synthesized by the 1,3-dipolar cycloaddition reaction using **1c** and the 8-(prop-2-ynoxy)quinoline. **QPA** and its precursor molecules were well characterized by <sup>1</sup>H and <sup>13</sup>C NMR, high-resolution mass spectroscopy (HRMS) and elemental analysis (Figs. S1–S4 in Supplementary Data).

The pillar[5]arene derivative, **QPA** has been studied for its interaction with various biologically relevant metal ions using fluorescence



Scheme 1. Synthesis of quinolone derivative of pillar[5]arene, **QPA**.

spectroscopy in aqueous acetonitrile (1:1). The **QPA** has been excited at 320 nm and followed its emission band at 400 nm. Among the eleven metal ions studied, **QPA** showed a significant decrease in fluorescence intensity upon interaction with  $\text{Fe}^{3+}$  (Fig. 1a). None of the other metal ions, viz.,  $\text{Na}^+$ ,  $\text{K}^+$ ,  $\text{Ca}^{2+}$ ,  $\text{Mg}^{2+}$ ,  $\text{Mn}^{2+}$ ,  $\text{Fe}^{2+}$ ,  $\text{Co}^{2+}$ ,  $\text{Ni}^{2+}$ ,  $\text{Cu}^{2+}$ , and  $\text{Zn}^{2+}$ , showed fluorescence changes except  $\text{Cu}^{2+}$  which shows minimal changes ( $\sim 7$  fold) upon the titration with **QPA** (Fig. 1b). The amount of fluorescence quenching observed during the titration of **QPA** with  $\text{Fe}^{3+}$  is  $\sim 31$  fold. Hence, **QPA** can be a selective sensor for the detection of  $\text{Fe}^{3+}$  among all the biologically relevant ions reported in this paper. The lowest amount of **QPA** required to detect  $\text{Fe}^{3+}$  in a sample using the

current fluorescence technique in aqueous acetonitrile solution is 157 ppm. The stoichiometry of the complex between **QPA** and  $\text{Fe}^{3+}$  were determined based on MALDI-TOF studies. The molecular ion peak observed at  $m/z = 781.32$   $\{m/5$  of  $3906.60$  of  $[\text{QPA} + 2\text{Fe}^{3+} + \text{ClO}_4]^{5+}$  indicates the 1:2 complex formation between **QPA** and  $\text{Fe}^{3+}$  (Fig. S5 in Supplementary Data). The isotopic peak pattern observed is characteristic for the presence of iron in the complex. The complex formation of **QPA** with  $\text{Fe}^{3+}$  has been further supported by UV-Vis spectroscopy and  $^1\text{H}$  NMR experiments (Figs. S6-S7 in Supplementary Data). Upon the addition of  $\text{Fe}^{3+}$  into a solution of **QPA** in  $\text{DMSO } d_6$ , the proton signals corresponding to triazole ring and quinoline

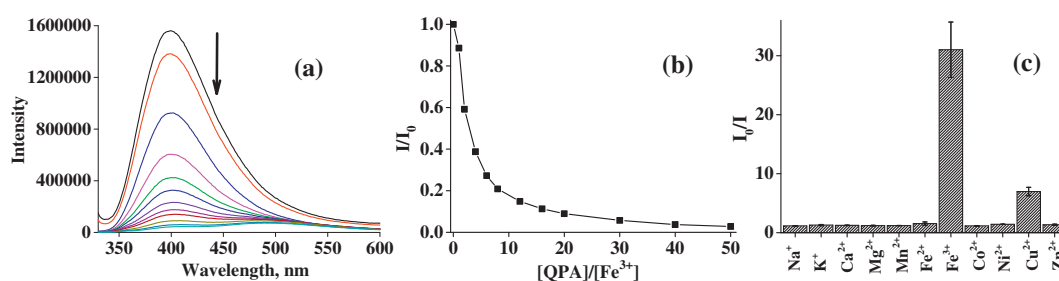


Fig. 1. (a) Fluorescence spectral traces obtained during the titration of **QPA** ( $10 \mu\text{M}$ ) with increasing concentrations of  $\text{Fe}^{3+}$ , (b) plot of relative fluorescence intensity with mole ratio of  $\text{Fe}^{3+}$ , and (c) histogram representing relative fluorescence intensity of **QPA** upon the addition of 50 equivalents of different metal ions.

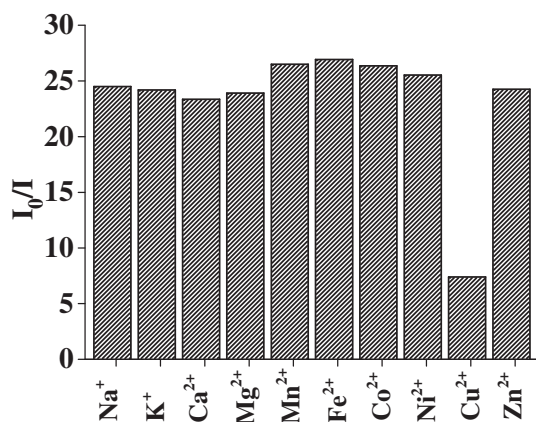


Fig. 2. Relative fluorescence intensity of **QPA** obtained during the addition of 50 equivalents of  $\text{Fe}^{3+}$  in the presence of 10 equivalents of  $\text{M}^{n+}$ .

experience considerable broadening along with marginal chemical shift. The changes observed in the  $^1\text{H}$  NMR experiments supporting the binding of  $\text{Fe}^{3+}$  with **QPA**.

A competitive metal ion titration has been carried out to demonstrate the efficiency of **QPA** to detect  $\text{Fe}^{3+}$  in the presence of other competing ions. An in-situ prepared mixture of **QPA** with 10 equivalents of metal ions other than  $\text{Fe}^{3+}$  was titrated with various concentrations of  $\text{Fe}^{3+}$  resulted in the fluorescence quenching of **QPA** indicating the selectivity of **QPA** towards  $\text{Fe}^{3+}$  over other ions (Fig. 2). During the competitive titration of  $\{\text{QPA} + \text{Cu}^{2+}\}$  with  $\text{Fe}^{3+}$ , the initial fluorescence intensity of the receptor was quenched  $\sim 4.2$  fold by the presence of  $\text{Cu}^{2+}$  and as a result, the total quenching fold obtained after the addition of  $\text{Fe}^{3+}$  was only 7.4 fold.

Since **QPA** showed selective quenching towards  $\text{Fe}^{3+}$  among other biologically relevant ions, we further explored the utility of in-situ prepared **QPA** and  $\text{Fe}^{3+}$  complex (**FeQPA**) as a secondary sensor for anions and amino acids. The **FeQPA** complex was prepared by mixing **QPA** and  $\text{Fe}^{3+}$  in a 1:10 ratio in aqueous acetonitrile solution. The stability of **FeQPA** complex in acidic and alkaline environment has been monitored by analysing the fluorescence spectral traces of **FeQPA** at different pH ranges. It has been found that **FeQPA** is stable in the pH ranges 3.5 to 10 (Fig. S8 in Supplementary Data).

In the detection of anions, the ensemble **FeQPA** was titrated with varying concentrations of halide ions, viz.,  $\text{F}^-$ ,  $\text{Cl}^-$ ,  $\text{Br}^-$  &  $\text{I}^-$ . The initial fluorescence intensity of the ensemble **FeQPA** has been quenched due to the presence of  $\text{Fe}^{3+}$ . During the titration with anions, the fluorescence band of **FeQPA** at 400 nm has been increased significantly upon the interaction with  $\text{F}^-$  and no changes were observed with other anions (Fig. 3). The reversal of fluorescence during the titration of **FeQPA** by the addition of  $\text{F}^-$  leads to the displacement of  $\text{Fe}^{3+}$  from the binding core of **FeQPA** and leaving the sensor **QPA** alone. The free  $\text{Fe}^{3+}$  forms a stable complex with  $\text{F}^-$  ( $[\text{FeF}_6]^{3-}$ ) and the fluorescence intensity of the **QPA** has been restored [43,44]. The chemosensor ensemble **FeQPA** exhibited  $\sim 4$  fold fluorescence enhancement upon interaction with  $\text{F}^-$ . Therefore, it clearly demonstrates the ability of **FeQPA** to detect  $\text{F}^-$  selectively among all the halide ions. The detection limit of  $\text{F}^-$  by **FeQPA** has been found to be 289 ppm. Absorption titrations were also carried out to support the secondary sensing of **FeQPA** with  $\text{F}^-$  and the corresponding results were summarised in the Fig. S9 of Supplementary Data. The displacement mechanism of **FeQPA** in the sensing of  $\text{F}^-$  has been further supported by  $^1\text{H}$  NMR titrations by adding 10 equivalents of  $\text{F}^-$  to an in-situ prepared complex of **FeQPA**. During the titration, the proton signals of triazole ring and the quinoline were marginally shifted and moved towards simple **QPA** (Fig. S10 in Supplementary Data). The regeneration of  $^1\text{H}$  NMR spectra of **QPA** upon the addition

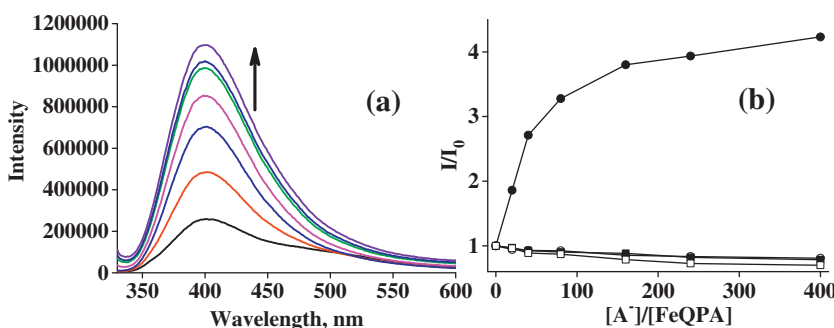


Fig. 3. (a) Fluorescence spectral traces obtained during the titration of in-situ prepared **FeQPA** with increasing concentrations of  $\text{F}^-$ , and (b) plot of relative fluorescence intensity of **FeQPA** with mole ratios of halides. Symbols corresponds to  $\bullet = \text{F}^-$ ,  $\circ = \text{Cl}^-$ ,  $\blacksquare = \text{Br}^-$ ,  $\square = \text{I}^-$ .

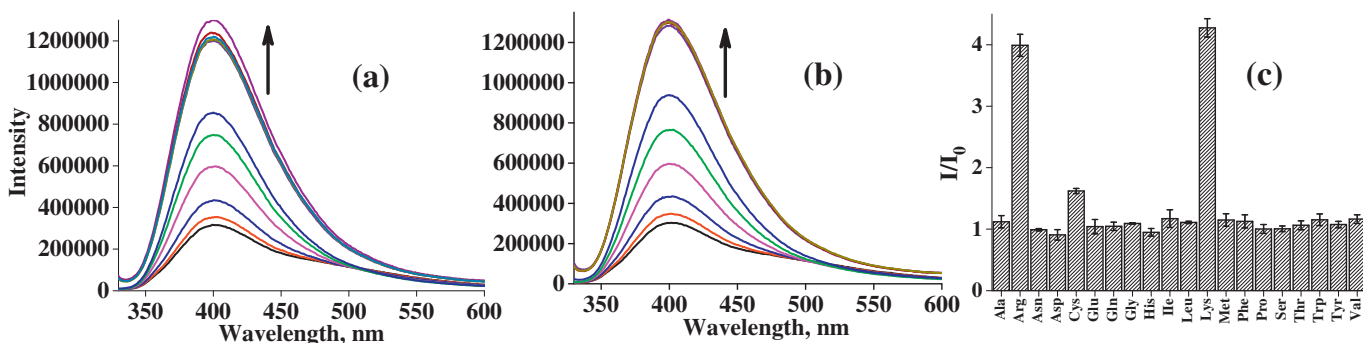


Fig. 4. Fluorescence spectral traces obtained during the titration of in-situ prepared **FeQPA** with increasing concentrations of (a) arginine, (b) lysine, and (c) histogram representing relative fluorescence intensity of **FeQPA** upon the addition of 50 equivalents of different amino acids.

of  $F^-$  supports the displacement of  $Fe^{3+}$  from the binding core of **FeQPA** complex.

Selective detection of amino acids using **FeQPA** has been investigated by fluorescence spectroscopy. The complex **FeQPA** has been titrated with increasing concentration of twenty naturally occurring amino acids and the corresponding fluorescence intensity was monitored. None of the amino acids, except arginine and lysine, have shown any change in the fluorescence intensity of **FeQPA** during the titration (Fig. 4). It indicates that **FeQPA** interacts selectively with arginine and lysine among all the amino acids reported in this paper. The fluorescence enhancement observed for arginine and lysine were 3.9 and 4.3 fold respectively (Fig. S11 in Supplementary Data). The **FeQPA** detects arginine and lysine among the naturally occurring amino acids to the lowest concentration of  $3.57 \times 10^3$  and  $3.17 \times 10^3$  ppm respectively. Similar to the detection of anions, a displacement mechanism is responsible for the fluorescence enhancement of the sensor molecule when it interacts with basic amino acids. During the absorption titration of **FeQPA** with arginine and lysine, the absorption band observed at 300 nm exhibited a marginal increase in the absorbance while the absorption band at 250 nm showed marginal decrease in the absorbance (Figs. S12–S13 in Supplementary Data). The displacement strategy for the detection of amino acids has been verified by  $^1H$  NMR titration. Upon the addition of 10 equivalents of lysine or arginine to a solution of in-situ prepared **FeQPA** resulted in the formation of  $^1H$  NMR spectra corresponds to free **QPA** (Fig. S14 in Supplementary Data). Therefore, **FeQPA** is a secondary sensor for lysine and arginine among twenty naturally occurring amino acids.

#### 4. Conclusions

In conclusion, quinoline appended pillar[5]arene, **QPA** selectively detects  $Fe^{3+}$  and its in-situ prepared  $Fe^{3+}$  complex, **FeQPA** exhibits secondary sensing towards  $F^-$ , and arginine and lysine. The sensing of  $Fe^{3+}$  has been monitored by the decrease in the fluorescence emission band of **QPA** at 420 nm while the detection of  $F^-$ , lysine and arginine have been observed by the fluorescence enhancement of **FeQPA** at 420 nm. The ion and molecular interactions have been monitored by fluorescence spectroscopy and the complexation was further supported by  $^1H$  NMR titration and MALDI-TOF experiments. The **QPA** detects  $Fe^{3+}$  to the lowest concentration of 157 ppm and **FeQPA**'s detection limits are 289,  $3.57 \times 10^3$  and  $3.17 \times 10^3$  ppm towards  $F^-$ , arginine and lysine respectively.

#### Acknowledgements

R.J. thanks the Department of Science and Technology (DST)-SERB India for Young Scientist Start-Up Research Grant (YSS/2015/001868). Thanks to Central Laboratory for Instrumentation and Facilitation (CLIF) at Kerala University for NMR analysis. R.J. acknowledges Jibin Raj R J (CLIF, Kerala University) for NMR data acquisitions.

#### Appendix A. Supplementary data

Supplementary data to this article can be found online at <https://doi.org/10.1016/j.saa.2019.117390>.

#### References

- [1] R.M. Duke, E.B. Veale, F.M. Pfeffer, P.E. Kruger, T. Gunnlaugsson, Colorimetric and fluorescent anion sensors: an overview of recent developments in the use of 1,8-naphthalimide-based chemosensors, *Chem. Soc. Rev.* 39 (2010) 3936–3953.
- [2] P.A. Gale, Anion receptor chemistry: highlights from 2008 and 2009, *Chem. Soc. Rev.* 39 (2010) 3746–3771.
- [3] R.S. Eisenstein, Iron regulatory proteins and the molecular control of mammalian iron metabolism, *Annu. Rev. Nutr.* 20 (2000) 627–662.
- [4] T.A. Rouault, The role of iron regulatory proteins in mammalian iron homeostasis and disease, *Nat. Chem. Biol.* 2 (2006) 406–414.
- [5] P. Aisen, M. Wessling-Resnick, E.A. Leibold, Iron metabolism, *Curr. Opin. Chem. Biol.* 3 (1999) 200–206.
- [6] M.D. Connie, C.W. Hsia, Respiratory function of hemoglobin, *N. Engl. J. Med.* 338 (1998) 239–247.
- [7] M.B. Murataliev, R. Feyereisen, F.A. Walker, Electron transfer by diflavin reductases, *Biochim. Biophys. Acta* 1698 (2004) 1–26.
- [8] M.F. Lucas, D.L. Rousseau, V. Guallar, Electron transfer pathways in cytochrome c oxidase, *Biochim. Biophys. Acta* 1807 (2011) 1305–1313.
- [9] N. Abbaspour, R. Hurrell, R. Kelishadi, Review on iron and its importance for human health, *J. Res. Med. Sci.* 19 (2014) 164–174.
- [10] X. Gao, J.L. Campian, M. Qian, X.-F. Sun, J.W. Eaton, *J. Biol. Chem.* 284 (2009) 4767–4775.
- [11] C.W. Siah, D. Trinder, J.K. Olynyk, Iron overload, *Clin. Chim. Acta* 358 (2005) 24–36.
- [12] X. Chen, Q. Zhao, W. Zou, Q. Qu, F. Wang, A colorimetric  $Fe^{3+}$  sensor based on an anionic poly(3,4-propylenedioxythiophene) derivative, *Sensors Actuators B Chem.* 244 (2017) 891–896.
- [13] J. Li, Q. Wang, Z. Guo, H. Ma, Y. Zhang, B. Wang, D. Bin, Q. Wei, Highly selective fluorescent chemosensor for detection of  $Fe^{3+}$  based on  $Fe_3O_4@ZnO$ , *Sci. Rep.* 6 (2016), 23558.
- [14] M. Kumar, N. Kumar, V. Bhalla, Thiocalix[4] crown based optical chemosensor for  $Fe^{3+}$ ,  $Li^+$  and cysteine: a  $Fe^{3+}/Li^+$  ion synchronized allosteric regulation, *Dalton Trans.* 42 (2013) 981–986.
- [15] F.M. Hinterholzinger, B. Rühle, S. Wuttke, K. Karaghiosoff, T. Bein, Highly sensitive and selective fluoride detection in water through fluorophore release from a metal-organic framework, *Sci. Rep.* 3 (2013) 2562.
- [16] B. Sui, B. Kim, Y. Zhang, A. Frazer, K.D. Belfield, Highly selective fluorescence turn-on sensor for fluoride detection, *ACS Appl. Mater. Interfaces* 5 (2013) 2920–2923.
- [17] M. Kleerekoper, The role of fluoride in the prevention of osteoporosis, *Endocrinol. Metab. Clin. N. Am.* 27 (1998) 441–452.
- [18] E.T. Everett, Fluoride's effects on the formation of teeth and bones, and the influence of genetics, *J. Dent. Res.* 90 (2011) 552–560.
- [19] G. Wu, Amino acids: metabolism, functions, and nutrition, *Amino Acids* 37 (2009) 1–17.
- [20] Y. Zhou, J. Yoon, Recent progress in fluorescent and colorimetric chemosensors for detection of amino acids, *Chem. Soc. Rev.* 41 (2012) 52–67.
- [21] M. Holecek, L. Sispera, Effects of arginine supplementation on amino acid profiles in blood and tissues in fed and overnight-fasted rats, *Nutrients* 8 (2016) 206–216.
- [22] S.D.S. Parveen, A. Affrore, K. Pitchumani, Plumbagin as colorimetric and ratiometric sensor for arginine, *Sensors Actuators B Chem.* 221 (2015) 521–527.
- [23] A.M. Pettiwala, P.K. Singh, Supramolecular dye aggregate assembly enables ratiometric detection and discrimination of lysine and arginine in aqueous solution, *ACS Omega* 2 (2017) 8779–8787.
- [24] K.A. Rawat, S.K. Kailasa, Visual detection of arginine, histidine and lysine using quercetin-functionalized gold nanoparticles, *Microchim. Acta* 181 (2014) 1917–1929.
- [25] R. Stanislavov, V.J. Nikolova, Treatment of erectile dysfunction with pycnogenol and L-arginine, *J. Sex Marital Ther.* 29 (2003) 207–213.
- [26] G. Wu, L.A. Jaeger, F.W. Bazer, J.M. Rhoads, Arginine deficiency in preterm infants: biochemical mechanisms and nutritional implications, *J. Nutr. Biochem.* 15 (2004) 442–451.
- [27] H. Yoshida, Y. Nakano, K. Koiso, H. Nohta, J. Ishida, M. Yamaguchi, Liquid chromatographic determination of ornithine and lysine based on intramolecular excimer-forming fluorescence derivatization, *Anal. Sci.* 17 (2001) 107–112.
- [28] D. Tomé, C. Bos, Lysine requirement through the human life cycle, *J. Nutr.* 137 (2007) 1642S–1645S.
- [29] D. Wu, A.C. Sedgwick, T. Gunnlaugson, E.U. Akkaya, J. Yoon, T.D. James, Fluorescent chemosensors: the past, present and future, *Chem. Soc. Rev.* 45 (2017) 7105–7123.
- [30] J. Li, D. Yim, W.-D. Jang, J. Yoon, Recent progress in the design and applications of fluorescence probes containing crown ethers, *Chem. Soc. Rev.* 46 (2017) 2437–2458.
- [31] D.G. Smith, I.L. Topolnicki, V. Zwicker, K.A. Jolliffe, E.J. New, Fluorescent sensing arrays for cations and anions, *Analyst* 142 (2017) 3549–3563.
- [32] R. Joseph, J.P. Chinta, C.P. Rao, Calix[4]arene-based 1,3-diconjugate of salicyllyl imine having dibenzyl amine moiety (L): synthesis, characterization, receptor properties toward  $Fe^{2+}$ ,  $Cu^{2+}$ , and  $Zn^{2+}$ , crystal structures of its  $Zn^{2+}$  and  $Cu^{2+}$  complexes, and selective phosphate sensing by the [ZnL], *Inorg. Chem.* 50 (2011) 7050–7058.
- [33] R.K. Pathak, V.K. Hinge, A. Rai, D. Panda, C.P. Rao, Imino-phenolic-pyridyl conjugates of calix[4]arene (L<sub>1</sub> and L<sub>2</sub>) as primary fluorescence switch-on sensors for  $Zn^{2+}$  in solution and in HeLa cells and the recognition of pyrophosphate and ATP by [ZnL<sub>2</sub>], *Inorg. Chem.* 51 (2012) 4994–5005.
- [34] K. Yang, Y. Pei, J. Wen, Z. Pei, Recent advances in pillar[n]arenes: synthesis and applications based on host-guest interactions, *Chem. Commun.* 52 (2016) 9316–9326.
- [35] J.-J. Chen, Y.-M. Zhang, H. Yao, T.-B. Wei, Pillararene-based fluorescent chemosensors: recent advances and perspectives, *Chem. Commun.* 53 (2017) 13296–13311.
- [36] Y. Wang, G. Ping, C. Li, Efficient complexation between pillar[5]arenes and neutral guests: from host-guest chemistry to functional materials, *Chem. Commun.* 52 (2016) 9858–9872.
- [37] M. Bojtar, A. Simon, P. Bombicz, I. Bitter, Expanding the pillararene chemistry: synthesis and application of a 10 + 1 functionalized pillar[5]arene, *Org. Lett.* 19 (2017) 4528–4531.
- [38] C. Sathiyajith, R.R. Shaikh, Q. Han, Y. Zhang, K. Meguellati, Y.-W. Yang, Biological and related applications of pillar[n]arenes, *Chem. Commun.* 53 (2017) 677–696.
- [39] J. Zhou, C. Yu, F. Huang, Supramolecular chemotherapy based on host-guest molecular recognition: a novel strategy in the battle against cancer with a bright future, *Chem. Soc. Rev.* 46 (2017) 7021–7053.

- [40] B. Shi, K. Jie, Y. Zhou, J. Zhou, D. Xia, F. Huang, Nanoparticles with near-infrared emission enhanced by pillararene-based molecular recognition in water, *J. Am. Chem. Soc.* 138 (2016) 80–83.
- [41] G. Yu, J. Zhou, J. Shen, G. Tang, F. Huang, Cationic pillar[6]arene/ATP host–guest recognition: selectivity, inhibition of ATP hydrolysis, and application in multidrug resistance treatment, *Chem. Sci.* 7 (2016) 4073–4078.
- [42] M. Irfan, S. Alam, N. Manzoor, M. Abid, Effect of quinoline based 1,2,3-triazole and its structural analogues on growth and virulence attributes of *Candida albicans*, *PLoS ONE* 12 (2017), e0175710.
- [43] M. Selvaraj, K. Rajalakshmi, Y.–S. Nam, Y. Lee, J.–W. Song, H.–J. Lee, K.–B. Lee, On-off-on relay fluorescence recognition of ferric and fluoride ions based on indicator displacement in living cells, *Anal. Chim. Acta* 1066 (2019) 112–120.
- [44] Y. Zhang, J. Su, Q. Li, W. Li, G. Liang, H. Li, H. Ma, Q. Lin, H. Yao, T. Wei, Novel fluorescent chemosensor for detection of F<sup>–</sup> anions based on a single functionalized pillar[5]arene iron(III) complex, *Chin. J. Chem.* 34 (2016) 1263–1267.